fDOI: 10.2507/34th.daaam.proceedings.xxx

ANALYTICAL CALCULATION AND EXPERIMENTAL MEASUREMENT COMPARISON OF BOLTED JOINT WITH INSERT FOR COMPOSITE SANDWICH PANEL

Katerina Kasova, Martin Melichar

This Publication has to be referred as: Kasova, K[aterina] & Melichar, M[artin] (2023). Analytical Calculation And Experimental Measurement Comparison of Bolted Joint With Insert For Composite Sandwich Panel, Proceedings of the 34th DAAAM International Symposium, pp.xxxx-xxxx, B. Katalinic (Ed.), Published by DAAAM International, ISBN 978-3-902734-xx-x, ISSN 1726-9679, Vienna, AustriaDOI: 10.2507/34th.daaam.proceedings.xxx

Abstract

This paper addresses the design of a structural joint involving a composite sandwich panel. In the context of composite sandwich panels, ensuring a robust connection between the panel and other structural elements is essential. Typically, these components are secured to the composite panel through bolted joint, making the bolted joint between the composite panel and the structural structure the focus of this paper. The primary focus here is on the design methodology of a pass-through insert with a hot bonded joint.

Keywords: Composite sandwich panel; Bolted joint; Experimental test; Insert; Carbon fibre.

1. Introduction

For composite sandwich panels, ensuring the connection between the panel itself and other structural elements is crucial. These components are primarily attached to the composite panel through bolts. The mechanics of composite joints constitute a complex discipline, and a dedicated study is necessary for designing specific joints. The central research question revolves around designing a bolted joint with a sandwich composite panel for selected material combinations.

This study delves into the intricate world of designing and assessing the integrity of these connections, which play a pivotal role in aerospace, construction, and various high-performance applications. While analytical calculations serve as a fundamental tool for initial design and estimation, their accuracy can be limited, particularly for complex material combinations. The incorporation of experimental measurements becomes essential to validate and refine these designs, ensuring they meet rigorous safety and performance standards. [1], [2].

By gaining a better understanding of the strengths and interplay between these two approaches, the main goal is to enhance the reliability and precision of bolted joints in composite sandwich panels. The insights gleaned from this analysis hold the promise of advancing engineering practices and, in the long run, contributing to the development of safer and more efficient designs across various industries. [2], [3].

A fundamental challenge with bolted joints involving composite sandwich panels is the compressive strength of the panel core. When a bolted joint is preloaded, the core can locally collapse, leading to joint failure (figure 1).

Fig. 1. Local core collapse in the bolted joint of a composite sandwich panel

Therefore, such joints are inadequate without additional reinforcing elements. In place of a bolted joint, an insert (Fig. 2) with high compressive strength must replace the core. Various materials are available for the insert, which must meet several essential criteria, including temperature resistance during panel curing, adequate compressive strength for preloading the joint, good adhesive properties, and more [4], [5], [6].

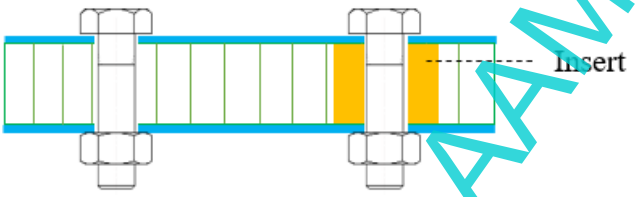

Fig. 2. Left bolted joint without insert; right bolted joint with insert

Inserts are categorized into two main types, depending on their attachment method within the sandwich panel:

- Hot-glued inserts are produced concurrently with the panel, with the skin/insert and core/insert bonded during the curing cycle of the skin.
- Cold-bonded inserts involve additional bonding of the insert after panel fabrication.

Other critical factors include whether the insert is pass-through or non-pass-through and the adhesive surface of the insert. Some standard insert types are illustrated in figure 3.

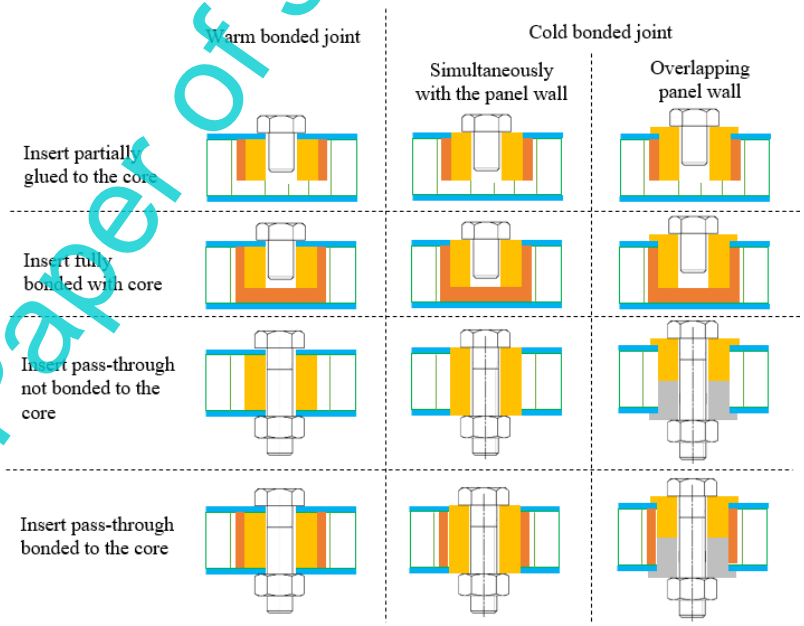

Fig. 3. Possible types of inserts and their method of insertion into the sandwich panel [7]

The design of a bolted joint with an insert is a highly intricate task influenced by various factors, including the materials of the sandwich panel, insert type and size, adhesive used, stress type, joint reliability, and more. Detailed

guidelines for designing a bolted joint with a bonded insert are provided in the publication "Space Engineering – Insert design handbook from the European Cooperation for space standardization" [8]. Another publication, "Validity check of an analytical dimensioning approach for potted insert load introductions in honeycomb sandwich panels" [6], compares analytical calculations with experimentally determined values for the design of a pass-through joint with an insert, revealing significant discrepancies. This underscores the necessity of supporting the fundamental design with experimental measurements for a given material combination. The knowledge derived from these publications was applied in designing the bolted connection with an insert, as discussed in the following section.

2. Analytical calculation of bolted join with insert

Given the complexity of this structural aspect, this paper exclusively focuses on the design methodology of the pass-through with a hot-glue bonded joint. This calculation deals with two design states for uniaxial tensile loads conditions:

1. Maximum stiffness condition, where there is no permanent deformation or composite panel failure.

The analytical calculation for the maximum allowable tensile load of the insert (equation 1) applies under several assumptions, such as neglecting the flexibility of inserts and adhesive, the elastic modulus of the skin being significantly greater than that of the core; $Ef \ll Ec$, the skin thickness t is several times smaller than the core thickness c; $t \ll c$, the distance between the edge of the insert and the embedded part of the panel is uniform (it is a circular sample). [9],[10]. Based on the aforementioned assumptions and the ECSS publication [7], the highest shear stress occurs at the insert/adhesive/core interface, as depicted in the figure 4.

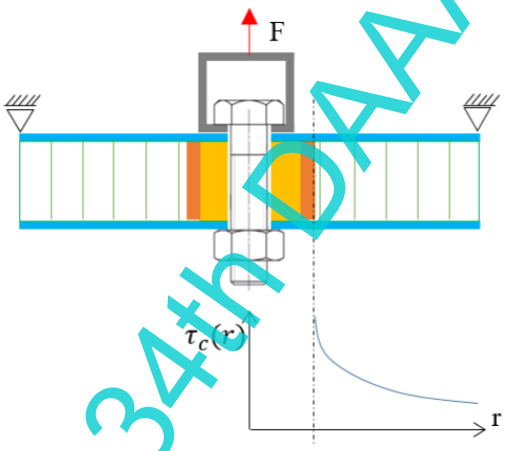

Fig. 4. Shear stress distribution in the panel section with insert

$$F_{cri} = 2\pi b_i d \tau_c \quad (1)$$

where F_{cri} is the critical load at which a failure occurs at the boundary between the insert and the core (N), b_i is the diameter of the insert including the adhesive layer (m), d is the mean distance of the skin (m), τ_c is the allowable shear load of the core (MPa).

2. Maximum tensile strength, where there is permanent deformation or composite panel failure (figure 5).

Shear failure of the skin occurs when the allowable shear stress of the skin is exceeded, as described in equation 2. The experimental measurement value of F_{kri-s} was lower than the calculated value because there is no ideal simultaneous failure of the outer and inner skin, as explained in equation 2.

$$F_{cri-s} = (\pi b_i t + \pi b_p t)\tau_{fmz} \quad (2)$$

where F_{cri-s} is the critical load at which the shear failure of the skin occurs when loading the bolted connection with the insert in tension (N), b_i is the diameter of the insert including the adhesive layer (m), b_p is the diameter of the washer (m), τ_{fmz} is the shear strength of the skin perpendicular to the plane of the skin (MPa).

The skin shear strength perpendicular to the plane of the skin is not a catalogue value and must be determined experimentally.

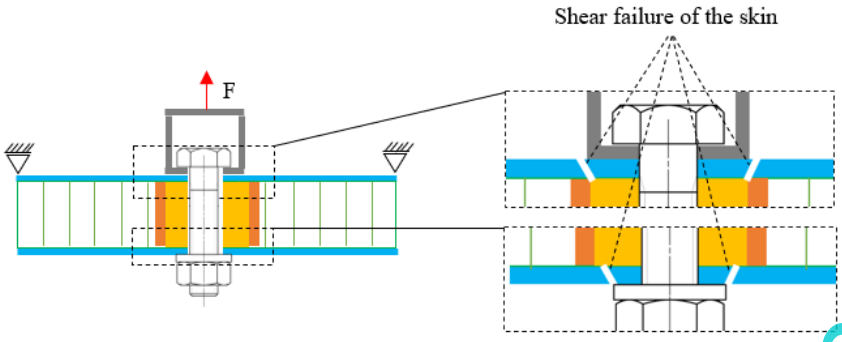

Fig. 5. Shear failure of the skin

3. Experimental measurement of skin shear strength

Experimental measurement of the shear strength of the skin in the direction perpendicular to the plane of the skin was conducted on 12 test specimens using various material combinations. Carbon fabric Toray 3K 200 Twill 2x2 was used for the skin material, while two different cores with different cell sizes were utilized for the core material. The 100x100 mm samples were produced via a two-cycle curing process in an autoclave, with IMP380FHC Black adhesive film used for the adhesive bond between the skin and core 250 g.m^{-2}.

Specimen	Material of skin	No. of layers in skin	Core	Core cell size (mm)	Panel height (mm)
Shear_P[4]_C[3,2/72]	Toray 3K 200 Twill 2x2	4	PAMG-XR-4.5-1/8-10-P-5056	3.2	21.8
Shear_P[4]_C[4.8/32]			PAMG-XR-2.0-3/16-07-P-5056	4.8	21.6
Shear_P[5]_C[3,2/72]		5	PAMG-XR-4.5-1/8-10-P-5056	3.2	22.2
Shear_P[5]_C[4.8/32]			PAMG-XR-2.0-3/16-07-P-5056	4.8	22.0

Table 1. List of test specimens for determining the shear strength of the skin

The shear strength tests were carried out under quasi-static loading at a speed of 5 mm.min^{-1} on a Zwick/Roell Z050 test rig, using a 25 mm push-through mandrel. A schematic of the test specimen arrangement is shown in the figure 6. The maximum shear strength of the skin perpendicular to the skin plane was determined from the maximum achieved load at the failure of the outer skin layer, as defined by equation 3.

$$\tau_{fmz} = \frac{F_{s-max}}{\pi d_{push} t} \tag{3}$$

where F_{s-max} is the maximum measured load during the test (N), d_{push} is the diameter of the shear mandrel (m), t is the thickness of the skin (m), τ_{fmz} is the shear strength of the skin perpendicular to the plane of the skin (MPa).

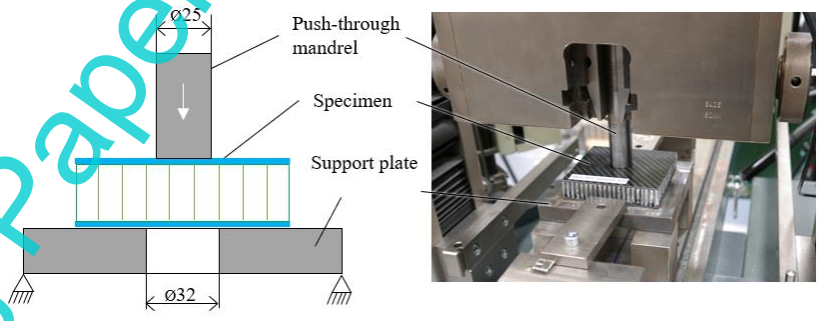

Fig. 6. Schematic of the specimen placement during the skin shear strength test

The results of the measurements were recorded in table 1. For each group of samples, the average value of the maximum load and the shear strength τ_{fmz} were calculated. Deviation in single specimen measurements is within 5% in most cases, except for Shear_P[4]_C[4.8/32], where the deviation is 7.3 %. It was evident from the measured values that the limit shear strength is significantly influenced by the core's stiffness, which provides support for the skin during testing.

sSpecimen	Maximum measured load (N)	Average maximum load (N)	Deviation of measured values from the average (%)	Thickness of the skin (mm)	Ultimate shear strength (MPa)
Shear_P[4]_C[3,2/72]_S[1]	6118.9	6101.8	2.7	1.04	**74.70**
Shear _P[4]_C[3,2/72]_S[2]	6011.4				
Shear _P[4]_C[3,2/72]_S[3]	6175.0				
Shear _P[4]_C[4,8/32]_S[1]	4968.6	4787.6	7.3	1.04	**58.61**
Shear _P[4]_C[4,8/32]_S[2]	4618.1				
Shear _P[4]_C[4,8/32]_S[3]	4776.1				
Shear _P[5]_C[3,2/72]_S[1]	7171.1	7243.6	3.7	1.3	**70.94**
Shear _P[5]_C[3,2/72]_S[2]	7414.2				
Shear _P[5]_C[3,2/72]_S[3]	7145.4				
Shear _P[5]_C[4,8/32]_S[1]	5435.8	5493.3	2.8	1.3	**53.80**
Shear _P[5]_C[4,8/32]_S[2]	5452.7				
Shear _P[5]_C[4,8/32]_S[3]	5591.4				

Table 2. Resulting measured values with specified shear strength

4. Experimental measurement of the strength of a pass-through bolted joint with insert

For the experimental measurement of the strength of the pass-through bolted joint with the insert, twelve test specimens were created. These specimens were identical to the ones used for shear strength measurements as shown in table 1. The sample dimensions were 120x120 mm, produced through a two-cycle curing process in an autoclave. IMP380FHC Black adhesive film was used to bond the skin and core, with an adhesive mass of 250 $g.m^{-2}$. The inserts were made of TECAPEEK CF30, with outer dimensions of 20 mm, height of 20 mm, and an inner diameter of 8 mm. Strength tests for the bolted joint with inserts were conducted under quasi-static loading conditions at a speed of 1 $mm.min^{-1}$ using a Zwick/Roell test rig Z050. The tests followed the ECSS standard as per ECSS-E-HB-32-22A. The schematic of specimen placement during the tensile strength test is presented in figure 7.

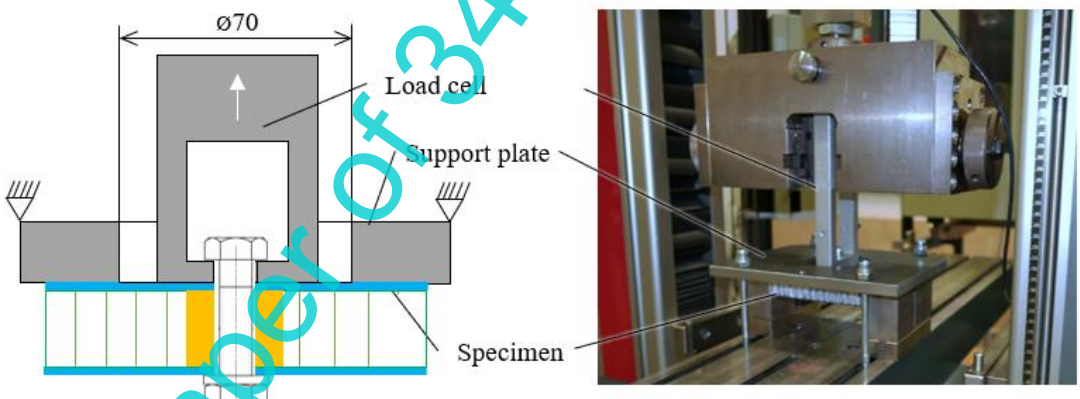

Fig. 7. Schematic of specimen placement during the tensile strength test of the insert

The recorded experimental measurement of the strength of the insert bolted connection for specimens Insert_P[4]_C[3,2/72] is shown in Graph 1. To determine the maximum stiffness, the dF/dy curve was plotted on graph 1. The measured force values at maximum stiffness for these specimens were approximately 60 % to 70 % of the proposed value of F_{cri} based on equation 1.

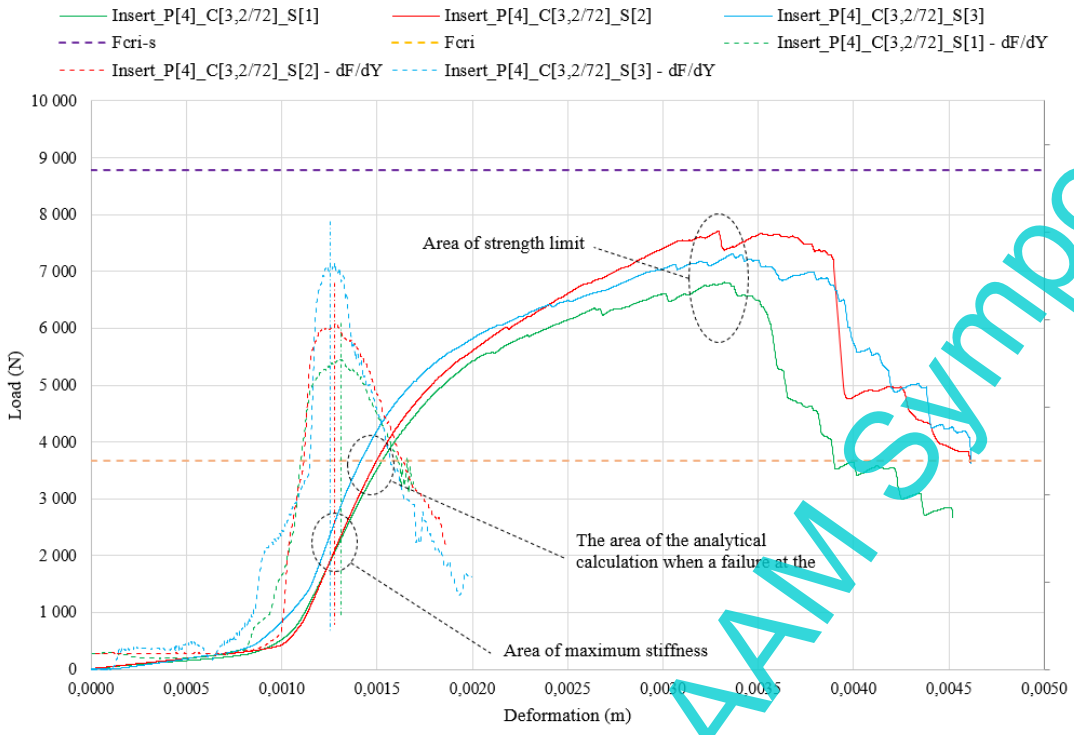

Graph 1. Experimental measurement of the strength of a bolted joint with an insert

The measured values are presented in table 3. The deviation of the measured values of the individual sample groups from the calculated average ranged from 5.9 % to 23.9 %. The term "uncertainty" refers to measurement deviation. [11] The deviation of the average critical load at the interface from the analytical calculation ranged from -17.2 % to -2.4 %. Using this deviation from the analytical calculation and the deviation from the measurement, a value was established for $F_{ckri\text{-}s0.7}$ according to equation 4.

$$F_{cri-s0,7} = 0{,}7\ F_{cri-s} \tag{4}$$

where $F_{cri-s0,7}$ is 70 % of the value F_{cri-s} (N), F_{cri-s} is the critical load at which the shear failure of the skin occurs when loading the bolted connection with the insert in tension (N).

Specimen	Critical loads at ultimate strength (N)	Average critical load at ultimate strength (N)	Deviation of measured values from the average (%)	F_{cri-s} (N)	Deviation F_{cri-s} from the average measured critical load (N)	Deviation F_{cri-s} from the average measured critical load (%)
Insert_P[4]_C[3,2/72]_S[1]	6808.7	7277.8	12.4	8786	- 1508.2	-17.2
Insert_P[4]_C[3,2/72]_S[2]	7714.2					
Insert_P[4]_C[3,2/72]_S[3]	7310.4					
Insert_P[4]_C[4,8/32]_S[1]	6838.7	6725.9	17.9	6894	- 168.1	-2.4
Insert_P[4]_C[4,8/32]_S[2]	7270.6					
Insert_P[4]_C[4,8/32]_S[3]	6068.3					
Insert_P[5]_C[3,2/72]_S[1]	9169.9	8999.6	5.9	10430	- 1430.4	-13.7
Insert_P[5]_C[3,2/72]_S[2]	9179.2					
Insert_P[5]_C[3,2/72]_S[3]	8649.7					
Insert_P[5]_C[4,8/32]_S[1]	6571.9	7182.5	23.9	7910	- 727.5	-9.2
Insert_P[5]_C[4,8/32]_S[2]	8286.0					
Insert_P[5]_C[4,8/32]_S[3]	6689.7					

Table 3. Final measured values of the critical load at the ultimate strength with deviation from the analytical calculation

The values of the specimens with the insert at maximum stiffness are provided in table 4. The deviation of the measured load concerning the load F_{cri} when failure occurs at the core-insert boundary was calculated, with deviations reaching up to 49.2 %.

Specimen	Load at maximum stiffness (N)	Average load at maximum stiffness (N)	F_{cri} (N)	Deviation F_{kri} from average measured load at maximum stiffness (N)	Deviation F_{kri} from average measured load at maximum stiffness (%)
Insert_P[4]_C[3,2/72]_S[1]	2261.3	2336.4	3648.3	-1342.0	-36.5
Insert_P[4]_C[3,2/72]_S[2]	2149.7				
Insert_P[4]_C[3,2/72]_S[3]	2598.0				
Insert_P[4]_C[4,8/32]_S[1]	952.4	981.3	872	102.9	11.7
Insert_P[4]_C[4,8/32]_S[2]	1061.1				
Insert_P[4]_C[4,8/32]_S[3]	930.4				
Insert_P[5]_C[3,2/72]_S[1]	1912.8	1879.5	3676.6	-1823.7	-49.2
Insert_P[5]_C[3,2/72]_S[2]	1685.3				
Insert_P[5]_C[3,2/72]_S[3]	2040.4				
Insert_P[5]_C[4,8/32]_S[1]	978.5	971.6	880.1	8[illegible]2	9.9
Insert_P[5]_C[4,8/32]_S[2]	1015.4				
Insert_P[5]_C[4,8/32]_S[3]	921.0				

Table 4. Final measured load values at maximum stiffness with deviation from the analytical calculation

5. Conclusion

This paper discusses the comparison of analytic calculations and experimental measurements of bolted joints with inserts in composite sandwich panels. The design of a bolted joint is a complex process influenced by various factors. To calculate the bolted joint with an insert, the shear strength rating of the skin was determined through experimental measurements, and these values are presented in table 2.

Experimental measurements were also conducted to assess the strength of the bolted joint with the insert perpendicular to the plane of the skin. The load values of specimens with insert at maximum stiffness are shown in Table 4. The deviation of the measured load with respect to the load F_{cri} when failure occurs at the core-insert boundary was calculated. This deviation amounts to a total of 49.2 %. This is due to the insufficient understanding of the deformation of the core at the boundary with the insert and the difficulty in determining the first core and skin failure. The resulting deviation was directly dependent on the shear stiffness of the core, with respect to the measured parameters.

Based on the presented results, it is evident that relying solely on analytical calculations is insufficient when designing bolted joint with inserts. For the optimal design of bolted joint with composite sandwich panels, it is imperative to incorporate experimental measurements of tensile properties and the specific insert joint. Without this experimental foundation, the precision of design based solely on analytical calculations would not meet the required standards.

The insights presented in this paper have led to a better understanding of the issues surrounding bolted joint with composite sandwich panels for specific material combinations. These findings enable the design of bolted joint for these specific material combinations with greater accuracy than could be achieved through analytical calculations alone.

In the future, these insights will be leveraged for the design of specific bolted joint with composite sandwich panels, followed by a retrospective verification through experimental measurements.

6. Acknowledgments

The article contribution has been prepared under project SGS-2022-007.

7. References

[1] Rana S. & Fangueiro R. (2016). Advanced Composite Materials for Aerospace Engineering: Processing, Properties and Applications. Woodhead Publishing, ISBN 978-0-08-100054-0, UK.

[2] Zenkert D. (1995). Introduction to Sandwich Construction. Engineering Materials Advisory Services Ltd., ISBN 978-0-947817-77-0, UK.

[3] Barbero E. J. (2010). Introduction to Composite Materials Design, Second Edition, 2 edition, CRC Press, ISBN 978-1-4200-7915-9, UK.

[4] Elmarakbi A. (2013). Advanced Composite Materials for Automotive Applications: Structural Integrity and Crashworthiness, Edición: 1, ISBN13:978-1-11842-36-8, Chichester, West Sussex, United Kingdom: Wiley.
[5] Bitzer T. N. (1997). Honeycomb Technology: Materials, Design, Manufacturing, Applications and Testing, Springer ISBN 978-9-401158-56-5, Netherlands.
[6] Zweben C. H. & Beaumont P. (2017). Comprehensive Composite Materials II, Elsevier, ISBN 978-0-081005-33-0, Netherlands.
[7] Wolff J.; Brysch M. & Hühne C. (2018). Check of an analytical dimensioning approach for potted insert load introductions in honeycomb sandwich panels, Compos. Struct., Available from: https://www.sciencedirect.com /science/article/abs/pii, Accessed on: 2022-08-13.
[8] https://ecss.nl/hbstms/ecss-e-hb-32-22a-insert-design-handbook (2011). ECSS E HB 32 22A Insert Design Handbook. ESA Requirements and Standards Division, Noordwijk, Netherlands, Accessed on: 2023-06-08.
[9] Campbell F. C. (2010). Structural Composite Materials, New ed. edition. Materials Park: ASM International, ISBN 9781615031405, Ohio.
[10] Jingsi W.; Badu O. A.; Yonchen T. & George A. R. (2014). Design, Analysis, and Simulation of an Automotive Carbon Fiber Monocoque Chassis. SAE Int. J. Passeng. Cars - Mech. Syst. 7(2):838-861, Available from: https://doi.org/10.4271/2014-01-1052, Accessed on: 2022-10-9.
[11] Kubatova, D. & Melichar, M. (2018). Uncertainty of Surface Measurement, Proceedings of the 29th DAAAM International Symposium, pp.1239-1248, B. Katalinic (Ed.), Published by DAAAM International, ISBN 978-3-902734-20-4, ISSN 1726-9679, Vienna, Austria DOI: 10.2507/29th.daaam.proceedings.179